Diagnostics and modeling of a macroscopic plasma display panel cell

Th. Callegari, R. Ganter, and J. P. Boeuf[a)]
CPAT, Université Paul Sabatier, 118 Route de Narbonne, 31062 Toulouse Cedex, France

(Received 27 March 2000; accepted for publication 7 July 2000)

A macroscopic plasma display discharge cell has been designed in order to more easily study the plasma evolution in dielectric barrier discharges occurring in the much smaller commercial ac plasma display panels (PDPs). The electrodes in the macrocell can be arranged in matrix or coplanar configurations. The dimensions of the cell are 100 times larger than those of typical PDP cells and the gas pressure is 100 times smaller. Although some of the properties of the discharge pulse obviously do not follow the classical similarity laws, we find that the macrocell is a very useful tool for improving our understanding of the discharge in a PDP cell. The large dimensions of the cell and the longer time scale because of the smaller pressure make the plasma diagnostics easier than in a real PDP cell. The results are presented here for discharges in pure neon at 5 Torr. Measurements of the time evolution of the current and imaging of the plasma with an intensified charge coupled device (ICCD) camera are presented in matrix electrode configurations and are compared with previously developed models. The experiment confirms the large power deposition in electron impact excitation of the gas atoms while the plasma spreads over the dielectric surface above the anode. The images obtained with the ICCD camera also show the existence of striations of the plasma near the dielectric surface which were not predicted by the models. Measured and calculated duration and shape of the current pulse are in reasonable agreement. © *2000 American Institute of Physics.* [S0021-8979(00)03820-2]

I. INTRODUCTION

In plasma display panels (PDPs) the visible light emitted in each picture element is produced by phosphors which are excited by UV photons from a microdischarge plasma. PDPs are now the ideal candidate for large area wall hanging televisions but improvements are still needed to increase the luminous efficiency and the contrast ratio of these displays. Numerical models of PDP discharge cells have been developed over the last few years and have helped understand the limited efficiency of these devices.[1–6]

Most commercial PDPs now use dielectric barrier discharges where the electrodes are covered with a dielectric layer and the voltage applied to the electrodes is alternative (ac PDP). The applied voltage frequency is on the order of 100 kHz, and the ''ON state'' of a discharge cell is characterized by a succession of transient discharge pulses. A cell is turned on by applying a voltage pulse above the breakdown voltage. After breakdown, the cell is kept in the ON state by applying a sustaining voltage below breakdown. This is possible because of the ''memory charges'' which are deposited by each discharge on the dielectric surfaces. At each half cycle of the applied voltage, the voltage induced by these memory charges adds to the voltage applied between the electrodes and a new discharge is initiated. This discharge extinguishes due to the charging of the dielectric and is reinitiated at the next half cycle.

PDPs with different electrode geometries have been developed. The two main electrode configurations are the matrix (or double substrate) structure and the coplanar (or single substrate) structure. In this article, we focus on dielectric barrier discharges with a matrix electrode geometry where the discharges are created at the intersections of column electrodes and row electrodes deposited on opposite parallel glass plates. In real PDPs, the discharges are confined between two parallel glass plates separated by a gas gap of about 100 μm. The thickness of the dielectric layer above the electrodes is on the order of 30 μm. The gas mixture contains a few percent of xenon (UV emitter) in neon or helium (to lower the breakdown voltage).

We have previously developed numerical models to describe the space and time evolution of the plasma during a PDP discharge pulse or a sequence of pulses.[1–5] These models have been used to analyze the power deposited in the gas by the discharge,[1,2,4] to study possible cross-talk effects between adjacent cells,[3] and to better understand the different addressing schemes.[5]

The purpose of this article is to confront the understanding of the plasma properties which has been obtained from these models, with detailed experimental measurements. Diagnostics on a real PDP cell is difficult (although possible, see, e.g., Refs. 7–11) because of the small dimensions and time scale. We have, therefore, built a macroscopic PDP cell which has the same geometry as a real cell but with much larger dimensions. We use a typical scaling factor of 100 in the cell dimensions and we operate the discharge at a pressure p 100 times lower than in a real cell (i.e., 5 Torr instead of 500 Torr). As is well known in discharge physics, discharges with the same (pd) (pressure times dimensions) can be ''similar'' under some conditions, and their time variations scale as (pt) (where t is the time). A discussion of the similarity laws applied to this problem is given in Sec. II.

a)Electronic mail: jpb@cpa01.ups-tlse.fr

Section III describes the experimental setup. The electrical properties of the plasma (current pulse, Paschen curve, voltage margin) are described in Sec. IV. with a discussion of the comparisons between experiments and models. Section V presents the time evolution of the plasma as observed with a charge coupled device (CCD) camera and predicted by the simulation.

II. SCALING LAWS

It is well known[12] that low current glow discharges having the same (pd) (pressure times gap length), have similar properties at the same (pt) (pressure multiplied by time), if the same voltage is applied to the electrodes. When p and d are changed while keeping the same pd and the same applied voltage (similar discharges), the following quantities are conserved:[12,13] J/p^2 where J is the current density. $n_{e,i}/p^2$ where n_e and n_i are the electron and ion densities, and E/p where E is the electric field.

These properties are the same for similar discharges at locations corresponding to the same px (x is the position in the gap) and at times corresponding to the same pt.

These classical scaling laws are valid when the only collisions which take place in the discharge are collisions between electrons and atoms in the ground state, and ions with atoms in the ground state. This situation generally occurs when the reduced current density, J/p^2, is relatively small.

In PDP conditions, the current density and the plasma density are low enough that collisions between charged particles and atoms in excited states do not play a significant role.[1,2,4] The only mechanisms which prevent the aforementioned scaling laws to be rigorously applicable to the electrical properties of the discharge are the recombination between electrons and positive (molecular) ions and the contribution of molecular ions to the current. The recombination loss in the plasma is proportional to the square of the plasma density and this nonlinearity invalidates the scaling laws when recombination is important.

In an ac PDP discharge one can distinguish two phases.

(1) *The current pulse*. In this phase (duration typically less than 100 ns at a few hundred Torr, recombination is not yet an important process, and most of the energy deposition in excited states takes places. This energy deposition occurs mainly through electron impact excitation and ionization from the ground state (the total power density is rather low and the density of excited states does not significantly affect the electron kinetics). Thus, the scaling laws are valid for this phase.

(2) *The afterglow*. In the afterglow phase, the current through the discharge is practically zero, as is the voltage drop across the gas gap. The plasma decays at a rate defined by recombination and ambipolar diffusion. It is clear that even for the same pd, the plasma density will decay faster (in units of pt) at higher pressure than at lower pressure because of the nonlinearity of the recombination loss term. For a given recombination coefficient, the relative importance of the recombination loss term, with respect to the ambipolar loss term, increases linearly with pressure. Moreover, in a rare gas mixture for PDPs, only recombination between electrons and molecular ions is significant and molecular ions are created by three body collisions (i.e., their density is significant at high pressure only). A simple estimation shows that recombination in a macrocell at 5 Torr would be negligible with respect to ambipolar diffusion while recombination and ambipolar diffusion are both important in a real PDP cell at 500 Torr. Therefore, the decay of the plasma does not follow the similarity laws and will be slower (in units of pt) in the macrocell experiment.

The most important phase in a PDP discharge is the current pulse phase since it is during that phase that the electrons are energetic enough to excite and ionize the gas.

We can, therefore, conclude that studying discharges at low pressure which are similar (i.e., same pd and same applied voltage as a function of pt) to PDP discharges can be very useful for validation of models of PDP's and can provide valuable information on the ways to improve the efficiency of plasma display. We have shown in previous articles that the efficiency in UV production in PDPs is closely related to the efficiency in the deposition of the electron energy in xenon excited states which occurs mainly during the current pulse.[1,4]

We have stated herein that recombination invalidates the similarity laws for the *electric* properties of the discharge during the afterglow. The kinetics of excited species during the afterglow also do not follow the similarity laws in PDPs. This is because three body collisions play an important role at a pressure of a few hundred Torr. An example of such three body collisions is a collision between an excited xenon atom and two rare gas atoms in the ground state leading to the formation of a molecular excited state. This means that the time evolution of the UV emission, as well as the relative importance of the emission from the resonant and from the excimer states, will not follow the similarity laws.

In summary, studying discharges similar to PDP discharges, but at lower pressure, is very useful because of the following.

(1) The energy deposition in xenon excitation occurs during the current pulse.

(2) The scaling laws should be valid during the current pulse.

(3) The UV emission efficiency in PDPs is directly related to the energy deposited in electron impact xenon excitation.

(4) Discharges similar to discharges in real PDPs but at lower pressure will have larger dimensions and larger time scales and will, therefore, be much easier to study experimentally. The electrode geometry and cell structure can also be changed more easily in the macrocell than in a real PDP cell. The macrocell is, therefore, well adapted to simple and low-cost optimization of the discharge properties and efficiency.

In this article we present results in pure neon. Results in xenon–neon mixtures will be reported in subsequent articles.

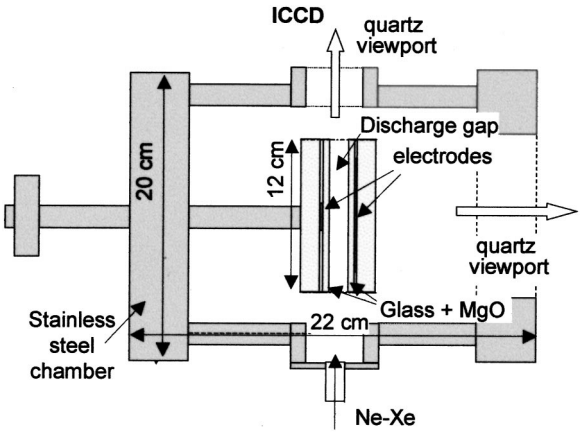

FIG. 1. Experimental setup.

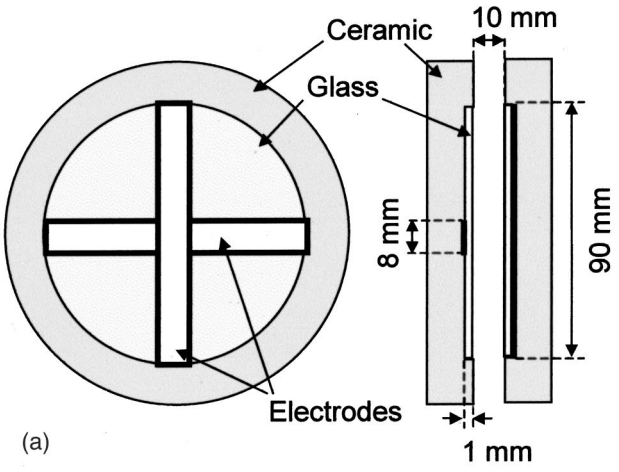

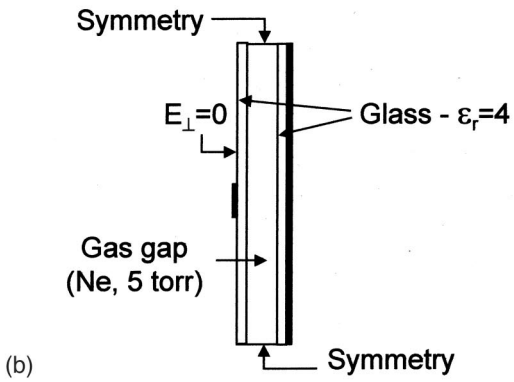

FIG. 2. (a) Electrode structure and applied voltage wave form. (b) Simulation domain is 2D cartesian (i.e., the discharge is supposed to be infinite and uniform along the direction perpendicular to the simulation domain). Vertical electrode is, therefore, equivalent to a plane in the 2D simulation.

III. EXPERIMENTAL SETUP AND MODEL CONDITIONS

A macrocell was built, with a geometry similar to that of PDP cell, but with dimensions about 100 times larger (i.e., typically 1 cm gas gap for matrix displays, and 1 cm electrode width). The operating pressure was about 100 times smaller than in PDPs i.e., in the 5 Torr range.

In these conditions, the time scale of the discharge evolution is 100 times larger than in a PDP cell so that measurements of the time dependent plasma properties are much simpler. Optical and electrical diagnostics were performed on this cell. We also used a two-dimensional (2D) self-consistent model[2–5] to study the successive discharge pulses in the cell. We will describe the experimental setup and the conditions of the simulations.

A. Experimental setup

An intensified CCD (Imax, Princeton Instruments) camera was used to look at the time evolution of the distribution of light emission by the discharge in matrix and coplanar PDP cells. The experimental setup is shown in Fig. 1.

The discharge cell is inserted in a 20 cm diameter stainless steel chamber. Several sets of electrodes were built and these can be arranged in matrix (see Fig. 2) or coplanar configurations. The gap length is on the order of 1 cm in the results presented here, but this dimension can be changed from a few millimeters to a few centimeters. In the results presented, the width of the electrodes is 8 mm and their length is 90 mm [see Fig. 2(a)]. The electrodes are covered with a 1 mm thick glass plate (relative permittivity ~4). The glass plates are covered with a 500 nm MgO film deposited by Thomson Plasma. The electrodes used in these experiments are in copper. Transparent, indium tin oxide (ITO) electrodes can also be used in order to allow CCD imaging or spectroscopy of the plasma through the electrodes.[14] A square wave voltage is applied between the electrodes. The frequency of the voltage is on the order of 150 Hz (in real PDPs, the voltage frequency is up to 100 kHz).

In the results presented herein, the CCD camera axis is perpendicular to the gas gap so that the images from the camera can be directly compared with the simulated results [see the simulation domain of Fig. 2(b)].

B. Conditions of the model and simulation domain

The model is identical to the one used in Refs. 2–5. It is a self-consistent 2D fluid model of the discharge where the space and time evolution of the electric potential, electron and ion density, and charge distributions on the dielectric layers are calculated. We assume a Cartesian, rectangular geometry and the simulation domain is shown in Fig. 2(b). This implies that the system is supposed to be infinite in the direction perpendicular to the simulation domain, and the model can yield current per unit length. The ionization rate is estimated using the local field approximation, and a constant value of the ratio of diffusion coefficient to mobility is assumed, as in Refs. 1–5. Recombination is negligible under these low pressure conditions.

The dimensions are the same as the macrocell dimensions shown in Fig. 2(a). The model assumes symmetry boundary conditions on the sides of the simulation domain perpendicular to the electrodes. This does not correspond to the experimental setup but we checked that this boundary condition does not have a strong influence on the results. On the sides of the domain which are parallel to the electrodes, the potential is imposed where there are electrodes, and the

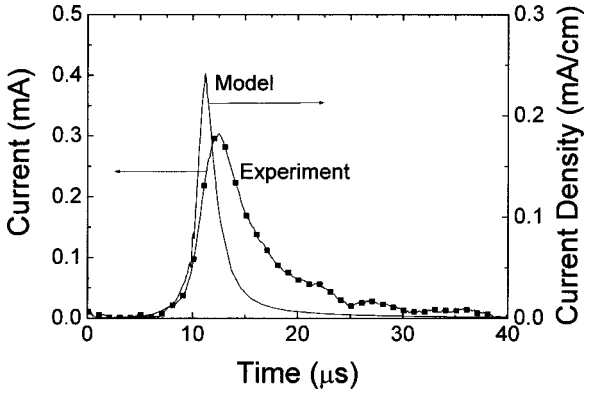

FIG. 3. Measured (symbols) and calculated current pulses in pure neon, 5 Torr, for a 1 cm gap length for the geometry and dimensions of Fig. 2 (standard case). Voltage pulse amplitude is 240 V and the voltage frequency is 150 Hz. Units for the model results are in milliamperes/centimeters (right-hand side axis). The capacitive current during the rise and decay of the voltage pulse has been subtracted from the measured and calculated total current.

electric field perpendicular to the domain is set to zero where there are no electrodes.

In the following results, calculations were performed by turning the cell on with a writing pulse. A large number of sustaining pulses were then simulated in order to reach a steady state sustaining regime.[3]

IV. ELECTRICAL CHARACTERISTICS: COMPARISONS BETWEEN EXPERIMENTS AND MODELS

The results presented were obtained in pure neon. The gap length was 1 cm and the gas pressure was 5 Torr. As previously mentioned, the width and length of the electrodes are 0.8 and 9 cm, respectively. The voltage frequency was typically 150 Hz, and the rise time of the voltage pulse was small enough in the model and experiments so that the discharge pulse occurred only during the plateau of the voltage pulse.

The experimental and simulated current pulses are presented and discussed in the first part of this section. Then, we briefly discuss questions related to the breakdown voltage and voltage margin.

A. Current pulse

In this section we present the measured and calculated current wave form. We compare the experimental and modeling results for a constant voltage amplitude. Then we show the effect of the applied voltage.

1. Current pulse shape

Figure 3 shows a typical comparison between a measured current pulse and a calculated one for a 2D geometry. The model calculations are performed for a square wave voltage with a very small rise time and the corresponding displacement current is not represented. The capacitive current has also been subtracted from the total measured current and is not represented in Fig. 3. This is done by first measuring the current for the same voltage wave form without discharge (e.g., in a vacuum). This current is then subtracted from the total current measured when the plasma is ON.

Three characteristic properties of the measured and calculated current pulses can be compared. These are the time delay between the beginning of the voltage pulse and the current peak, the rise time, and the decay time of the current pulses. The delay time depends strongly on the electron and ion density at the beginning of the pulse, i.e., on the charge remaining in the gap volume from the previous discharge pulse. We know that the model does not accurately describe the afterglow of the discharge pulse and we will not compare the time delays obtained in the experiments and in the model. The afterglow in these low pressure conditions is dominated by ambipolar diffusion and, since the model does not self-consistently calculate the electron energy during the afterglow, we do not expect to have a good estimation of the charges remaining in the gap at the end of a discharge pulse. While the initial number of electrons and ions in the gap at the beginning of a pulse obviously affect the time delay, it has little or no influence on the shape of the current pulse (this has been checked in both model and experiments, by changing the voltage frequency between 100 Hz and 1 KHz. Figure 3 shows that the calculated and measured rise times are in rather good agreement. The decay time of the current is shorter in the model. The half width of the current pulse is about 5 μs in the experiment and 2.5 μs in the simulation. The magnitude of the measured and calculated current pulses cannot be directly compared because the model provides a current per unit length rather than a current. Since the electrode width is on the order of 1 cm and the calculated peak current density is about 0.25 mA/cm (see Fig. 3), we estimate that the peak current predicted by the model to be on the order of 0.25 mA, which is not far from the measured peak current.

The discrepancy between the predicted and measured decay time of the current can be analyzed as follows. The shorter calculated pulse duration can be due to (a) the local field approximation in the model, (b) the assumption of constant D/μ in the model of electron transport (see a discussion of the model approximation in Refs. 2 and 4), (c) inaccuracies in transport coefficient such as ion drift velocities, (d) uncertainty in secondary emission coefficient, and (e) the fact that the model is only two-dimensional. These five hypotheses for the observed discrepancy between model and experiments are discussed further.

The local field approximation tends to overestimate the proportion of ions created in the sheath. Due to nonlocal effects, some ions are generated in the low field region of the glow and this can slow down the collection of positive ions on the surface above the cathode. We have observed in previous work[2] that including nonlocal effects (by using a hybrid fluid—Monte Carlo simulation for electrons) leads to a slightly longer pulse duration.

The assumption of constant D/μ in the electron momentum transport equation leads to an overestimation of the ambipolar diffusion coefficient during the afterglow. D/μ is taken constant and equal to 1 V for the electrons in the calculations. The electron temperature should actually thermalize rather quickly during the afterglow and we can, therefore, expect the model to predict a shorter duration of the afterglow than observed in the experiment. In order to check the

effect of D/μ, we did some calculations with lower values of D/μ, or with a D/μ decreasing during the afterglow. The results show that although this has some effects on the duration of the afterglow, it does not significantly affect the shape of the current pulse. This is because there is no current collection during the afterglow, which is controlled by pure ambipolar diffusion (the dielectric surfaces are charged and the potential drop in the gas gap is zero).

We also tried to estimate the effect of uncertainties in the values of the neon ion mobility. We could obtain a calculated current duration close to the measured one by artificially decreasing the neon ion drift velocity by more than a factor of two. We think that the uncertainty of our data of ion mobility in pure neon is much less than this, so the difference between measured and calculated current pulse duration is probably not due to inaccuracies in ion mobility.

The secondary emission coefficient γ and its dependence on E/p are not well known (see the brief discussion in Sec. IV B). We performed simulations with dependencies of γ on E/p similar to those measured in recent experiments,[15] and found that the exact shape and duration of the current pulse are indeed quite sensitive to the field dependency of the γ coefficient. This point will be investigated in detail in future work.

Another source of differences between the model and the experiment is the fact that the model assumes a 2D cartesian geometry. This means that the discharge is supposed to be infinite in the direction perpendicular to the simulation domain. This tends to overestimate the equivalent capacitance of the dielectric layer above the vertical electrode (electrode parallel to the side of the simulation domain, see Fig. 2). On the other hand, due to the 2D nature of the simulation, the plasma cannot spread along the horizontal left electrode in Fig. 2. This leads to a faster drop of the voltage across the gap and, therefore, to a shorter current pulse duration. In order to compensate for the larger equivalent capacitance of the dielectric layer induced by the 2D nature of the model, we performed calculations with the same geometry, but with a dielectric permittivity lower than in experiments. Decreasing the permittivity by less than a factor of 2 led to a calculated current pulse wave form in excellent agreement with the experiments. Therefore, the fact that the model is only two-dimensional also tends to shorten the duration of the current pulse. Similar conclusions were obtained in the work of Verasingam *et al.*,[16] where the authors compare calculated and measured current pulses in a PDP discharge in a helium–xenon mixture.

2. Current pulse as a function of voltage

Figures 4(a) and 4(b) respectively show the measured and calculated current pulse wave forms for different values of the applied voltage. As expected, the time delay increases and the current peak decreases when the applied voltage decreases. The half width of the current pulse is only slightly affected by the voltage. As previously described, the model predicts pulse durations about half of those measured.

The minimum operating voltage is larger in the simulation than in the experiment (220 V instead of about 200 V in the experiments). The minimum and maximum operating voltage (i.e., the ''voltage margin'' of the cell) depend strongly on the secondary emission coefficient as discussed below.

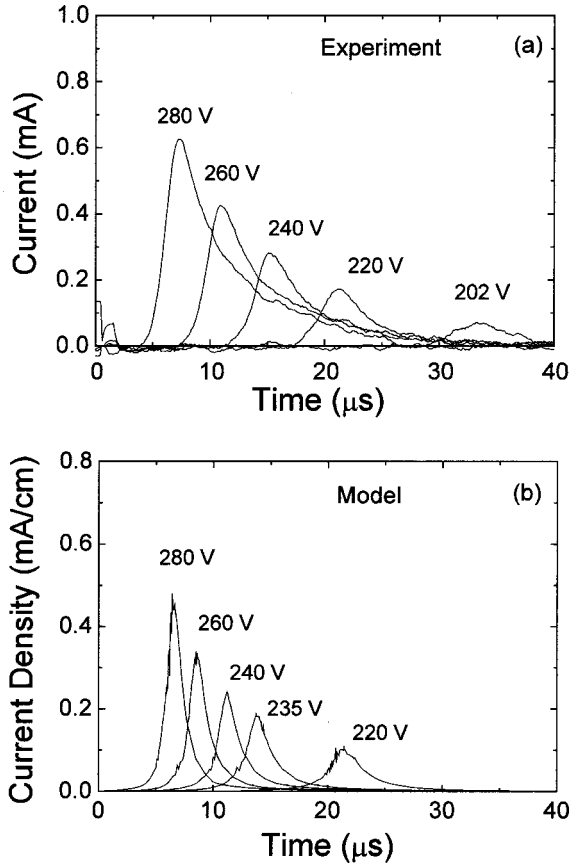

FIG. 4. (a) Measured current pulses for different voltage amplitudes (conditions of Fig. 3). (b) Calculated current pulses for different voltage amplitudes (conditions of Fig. 3).

B. Paschen curves, voltage margin, and MgO layer

In spite of some previous work,[15] the secondary electron emission coefficient γ due to ion impact on MgO is not accurately known and a complication is that it apparently depends very much on the state of the surface. In the simulation we used a constant value of γ (γ=0.11) which was adjusted to obtain a good agreement between calculated and measured breakdown voltage for a pressure of 5 Torr and a gap length of 1 cm. The secondary emission coefficient is actually a function of the ion energy and, therefore, of the value of the reduced electric field E/p on the MgO surface. The reduced electric field along the MgO surface varies over a large range during the current pulse (variations between a few volts/centimeters/Torr at the end of the current pulse, and typically 200 V/cm/Torr at the time of peak current). Variations of γ by a factor larger than 2 or 3 in this range of variations of E/p would not be surprising.

Plasma display cells can be characterized by the operating margin which is defined as the voltage range between the minimum sustaining voltage and the maximum sustaining voltage. The minimum sustaining voltage is the amplitude of the square wave voltage below which the discharge can no

longer be sustained. The maximum sustaining voltage is close to the breakdown voltage and its variation with pd give the Paschen curve. If the square wave voltage applied to the electrodes is above this voltage, it is no longer possible to control the ON and OFF states of the cell (the cell is always in the ON state).

In this work, no particular care was taken in preparing the MgO layer and we find that the measured breakdown voltage is larger than in real PDPs. As previously stated, the secondary emission coefficient for neon ions on MgO was adjusted to obtain a good match between calculated and measured breakdown voltage at $p=5$ Torr and $d=1$ cm. The adjusted value $\gamma=0.11$ is lower than expected for neon ions on a MgO layer (see, e.g., Ref. 17) and this suggests that the MgO surface was not properly prepared. The heating of the layer is especially important and in the industrial process of PDP fabrication, the surface is heated at 300 °C for several hours.[18] The MgO surface in the experiment was prepared by electron-beam evaporation on the glass substrate, and was subsequently heated to 200 °C for 24 h in the vacuum chamber.

Since the goal of this article was mainly to compare model predictions with measurements, the quality of the MgO layer was not an important issue. However, work is continuing to improve the quality of our MgO surface and to accurately determine the variations of the secondary emission coefficient of neon ions on MgO as a function of E/p.

V. SPACE AND TIME EVOLUTION OF THE PLASMA

In this section we present images of the space and time evolution of the plasma viewed in a direction perpendicular to the electrode gap (see Fig. 2) from both experiments and the model.

The experimental images have been obtained with a time exposure of 50 ns of the CCD camera at different times during a current pulse, and integrated over a large number of pulses. No filter was used in this experiment so the images correspond to the total light emitted by the discharge modified by the sensitivity spectrum of the CCD. Most of the light is, however, expected to come from visible red-orange photons from neon, with a strong peak at 585.2 nm.[19] Since the decay of the excited states leading to this emission is rather fast,[19] we expect these images to provide a good estimate of the space and time evolution of the electron impact excitation rate of the neon atoms.

The model directly provides the space and time evolution of the excitation rate of neon, and the calculated distribution of neon excitation rate can, therefore, be compared qualitatively with the images from the experiments.

A. CCD camera imaging

An example of the space and time variation of the light emitted by the discharge as measured by the CCD camera can be seen in Fig. 5. The conditions are: pure neon: 5 Torr gas gap; 1 cm, applied voltage amplitude; 243 V, and voltage frequency; 200 Hz.

In Fig. 5, the left-hand side ''horizontal'' electrode is the cathode, and the right-hand side ''vertical'' electrode is the anode. From Fig. 5, we can describe the breakdown, plasma formation, expansion, and decay as follows.

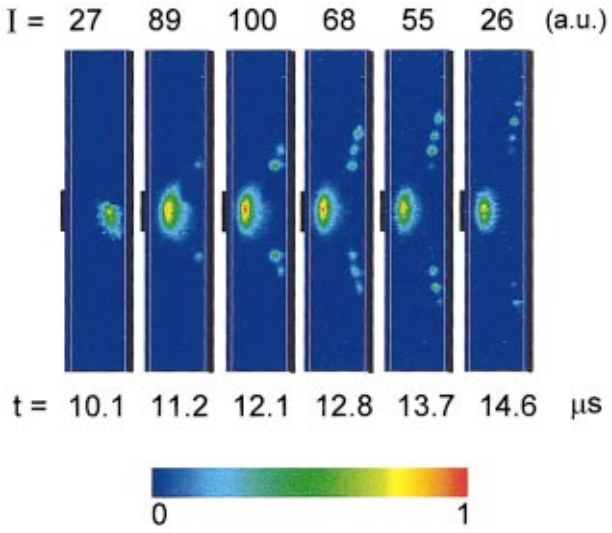

FIG. 5. (Color) ICCD side view images of the plasma at different times when the vertical electrode is the anode in the geometry of Fig. 2 in pure neon, 5 Torr. The amplitude and frequency of the voltages are 245 V and 150 Hz, respectively.

(1) The plasma forms above the dielectric surface in front of the anode.
(2) As the plasma expands, the ion sheath contracts above the dielectric surface in front of the cathode. The plasma-sheath boundary is close to the maximum of plasma emission along the discharge axis since the emission in a negative glow plasma is maximum at the end of the sheath, where the electrons release their energy in inelastic collisions.
(3) As the sheath contracts, the plasma on the anode side tends to spread along the dielectric surface.
(4) The spreading of the plasma along the dielectric surface above the anode is accompanied by the formation of striations in the emitted light.
(5) The light emission decays on the same time scale as the current.

The minimum sheath length can be estimated from the position of the maximum of light emission on the cathode side of the discharge. We obtain a value on the order of 2 mm for the minimum sheath length. Using the aforementioned scaling laws, this corresponds to a sheath length of 20 μm in the conditions of a real PDP cell (at 500 Torr, 100 μm gap length).

The description of the plasma formation and decay from the CCD camera images is very similar to what was obtained in previous modeling work.[3] We compare, in detail, the space and time evolution of the calculated neon excitation rate with the measured light emission from the plasma.

B. Comparisons with the simulation

Calculations were performed with the 2D fluid model in the same conditions as in the experiment previously described. The simulation results are shown in Fig. 6. Note that

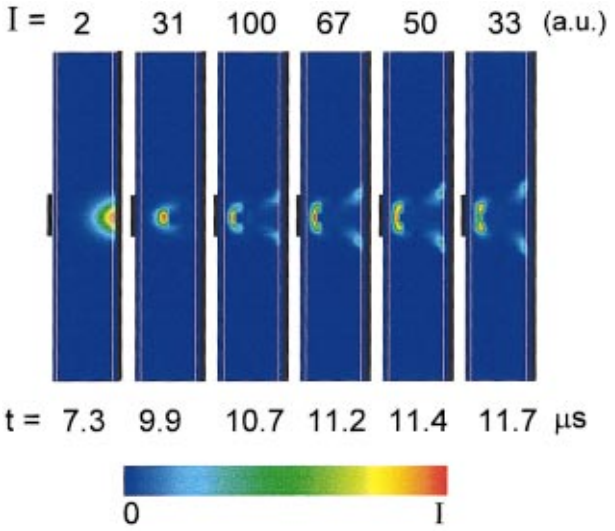

FIG. 6. (Color) Results from the 2D simulations in the conditions of Fig. 5.

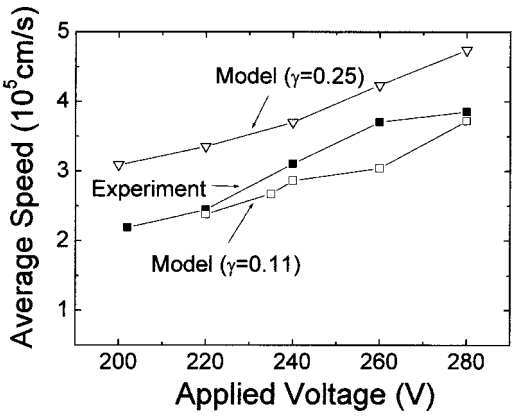

FIG. 7. Measured and calculated plasma expansion (or sheath contraction) velocity as a function of the applied voltage pulse amplitude (pure neon, 5 Torr, geometry of Fig. 2).

the model results in Fig. 6 show the total power deposited by electrons in neon excitation, while the measurements of Fig. 5 display the emission intensity as seen by the CCD camera and integrated over the whole spectrum (neon red-orange emission is dominant in these conditions).

The calculated power deposition in neon excitation and measured emission intensity are in good qualitative agreement, although some features are different. The comparison between model and experiment is summarized as follows.

(1) The simulation shows that, as in the experiments, the plasma first forms on the dielectric surface above the anode.

(2) The maximum of electron excitation then moves from the anode to the cathode. The velocity of the plasma expansion which can be deduced for model and experiments are in good agreement, as described in detail in the next section.

(3) The spreading of the plasma above the dielectric surface in front of the anode observed in the measurements is also predicted by the numerical models (see Fig. 6 and Ref. 3). As discussed in previous papers,[2–5] the spreading of the plasma along this surface is due to the charging of the dielectric. The electrons first charge the dielectric surface around the discharge axis. This leads to a decrease of the potential at that location. The electrons which continue to flow from the plasma to this surface, are therefore deflected along the surface by the electric field which is induced by the potential gradient. This electric field parallel to the surface is large enough to heat the electrons, leading to strong electron impact excitation of neon atoms. The spreading of the plasma along the surface is accompanied by intense light emission on a larger distance in the experiment than in the simulation.

(4) The simulation results do not reproduce the striations appearing in the experiments. This is not surprising since the model is based on the local field approximation and can, therefore, not describe phenomena associated with spatial relaxation of the electron energy. Such phenomena may be responsible for the observed striations and are characteristic of positive column plasmas.[13]

(5) The duration of the measured light emission and the calculated electron excitation are consistent with the measured and calculated current pulse durations.

The minimum sheath length which can be deduced from the position of the maximum power deposition in the simulation of Fig. 5 (about 1 mm) is shorter than in the experiments (which is on the order of 2 mm). This discrepancy is partially due to the fact that the model assumes local ionization and the maximum of gas excitation occurs inside the sheath instead of in the glow (see the comparison between fluid and hybrid model in Ref. 2).

C. Plasma expansion velocity

The velocity of the plasma expansion along the discharge axis can be deduced from the measurements and calculations. This velocity can be estimated by measuring the velocity of the peak of light emission or electron excitation observed in the experiment or deduced from the model, respectively. This velocity is plotted as a function of applied voltage in Fig. 7 for both the model and the experiment. The velocity is obtained by measuring the time taken by the peak of plasma emission (or excitation, in the model) to move from a position 1 mm above the dielectric layer on the anode side, to a position 3 mm above the dielectric layer on the cathode side.

We obtain a velocity of a few 10^5 cm/s in both the model and the experiments, which increases, as expected, with the applied voltage. The plasma expansion velocity is not directly related to the ion velocity. It is, rather, associated with volume ionization and secondary emission phenomena. The calculated plasma expansion velocity increases with increasing secondary emission coefficient. The better agreement between experiments and model for $\gamma=0.11$ is consistent with the fact that this value of γ gives the best fit between calculated and measured breakdown voltages at $p=5$ Torr and $d=1$ cm. The good agreement between the experiment and the model shows that the model includes the main physical phenomena which control the plasma expansion. This also indicates that photoemission (which is not included in the

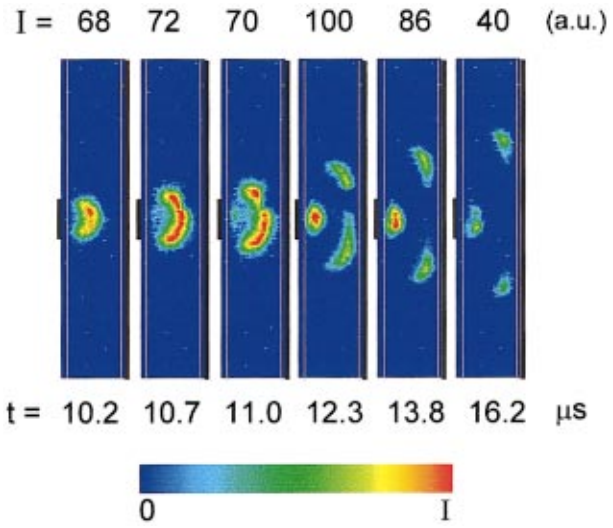

FIG. 8. (Color) ICCD side view images of the plasma at different times when the vertical electrode is the cathode in the same conditions as Fig. 5.

simulation) does not seem to play an important role in our conditions. Significant photoemission would substantially increase the plasma expansion velocity.

D. Case of a vertical cathode

The results in Figs. 5 and 6 were obtained for current pulses where the anode is vertical (right-hand side electrode in Figs. 5 and 6) and the cathode is horizontal, perpendicular to the simulation plane.

In Fig. 8 we present CCD images obtained for the other half cycle of the applied voltage i.e., when the vertical electrode is the cathode and the horizontal electrode is the anode. Figure 8 displays CCD images obtained in the same conditions as Fig. 5. We see, as in Fig. 5, the plasma formation next to the anode (left-hand side electrode) and its expansion toward the cathode. The curvature of the sheath due to the cross electrode geometry appears clearly in Fig. 8. After the current peak, the sheath region continues to spread along the cathode.

The simulation results (not displayed here) are in good qualitative agreement with the pictures in Fig. 8. As before, we find that the spreading of the plasma along the right-hand side vertical electrode predicted by the model is not as important as in the experiment.

VI. CONCLUSION

A macroscopic plasma display panel discharge cell has been studied experimentally and the measurements were compared with the results of a previously developed model of PDP cells. The geometry of the cell is similar to the geometry of a real PDP cell in a matrix electrode configuration, but with dimensions 100 times larger than those of a real cell. The gas pressure (5 Torr neon) was 100 times lower than in a real cell. Electrical measurements and imaging of the plasma development in the cell have been performed and compared with the results from the simulations.

The comparisons of the electrical characteristics of the cell show that the numerical model tends to underestimate, by a factor of 2, the current pulse duration when the geometry of the 2D model is identical to the experimental geometry projected in a plane containing the discharge axis and parallel to one of the electrodes. The model is only two-dimensional, and this tends to increase the real capacitance between the plasma and this electrode. A better agreement between calculated and measured current pulse duration can be obtained when this capacitance is artificially decreased in the simulation. Other reasons for the discrepancy between model and experiment can be due to the E/p dependence of the secondary emission coefficient which is not included in the simulation, or to nonlocal effects.

Comparisons between images of the plasma evolution obtained with a CCD camera are in excellent qualitative agreement with the predictions of the model for the space and time evolution of the electron impact excitation rate of neon. The calculated velocity of the plasma expansion (a few 10^5 cm/s) is close to the measured one. Both calculations and measurements show that the plasma spreads along the dielectric surface above the anode. The spreading is associated with the charging of the dielectric surface and with the potential gradient parallel to the surface which is induced by the charging. This potential gradient is large enough to provide energy to the electrons sufficient to induce excitation of the gas and a significant emission is detected by the camera and predicted by the model during the electron spreading along the surface. The model, however, does not reproduce the formation of striations of the light emitted which are seen in the experiments.

The reasonable agreement between the model results and experiments confirms that the model captures the important properties of the plasma formation in the cell and can be used efficiently to help design and optimize plasma display cells.

ACKNOWLEDGMENTS

This work has been supported partly by Thomson Plasma and by the French Ministry of Research and Technology in the frame of the RMNT program. The authors would like to thank L.C. Pitchford, J. Galy. Ph. Guillot, A. Ricard, and N. Sadeghi for helpful suggestions and comments, and R. Eyraud and J. L. Bonneval for their help in designing and building the experimental cell. The authors also want to thank L. Tessier and H. Doyeux from Thomson Plasma for their interest in this work.

[1] J. Meunier, Ph. Belenguer, and J. P. Boeuf, J. Appl. Phys. **78**, 731 (1995).
[2] J. P. Boeuf, C. Punset, A. Hirech, and H. Doyeux, J. Phys. IV **7**, C4-3 (1997).
[3] C. Punset, J.-P. Boeuf, and L. C. Pitchford, J. Appl. Phys. **83**, 1884 (1998).
[4] J. P. Boeuf, Th. Callegari, C. Punset, and R. Ganter, International Display Workshop IDRC, Seoul, S. Korea 1998, Vol. 18, pp. 209–220.
[5] C. Punset, S. Cany, and J. P. Boeuf, J. Appl. Phys. **86**, 124 (1999).
[6] S. Rauf and M. J. Kushner, J. Appl. Phys. **85**, 3460 (1999).
[7] H. S. Jeong, J. H. Seo, C. K. Yoon, J. K. Kim, and K.-W. Whang, J. Appl. Phys. **85**, 3092 (1999).
[8] M. Sawa, T. Tsutsumi, K. Yoshida, and H. Uchiike, SID International Symposium, 1999, Kobe, Japan pp. 284–287.

[9] T. Shiga, K. Igarashi, and S. Mikoshiba, International Display Workshop IDW '98, pp. 487–490.
[10] T. Yoshioka, A. Okigawa, L. Tessier, and K. Toki, International Display Workshop IDW '99, Sendai, Japan, pp. 603–606.
[11] L. F. Weber, 1999 International Display Research Conference (EuroDisplay '99), Berlin, Germany, September 1999 (unpublished) (see http://www.plasmaco.com/LarryPaper/paper.html).
[12] A. von Engel, *Ionized Gases* (Clarendon, Oxford, 1965).
[13] Yu. Raizer, *Gas Discharge Physics* (Springer, Berlin, 1991).
[14] Th. Callegari, R. Ganter, Ph. Guillot, J. Galy, and J. P. Boeuf, International Display Workshop IDW '99, Sendai, Japan, pp. 663–666.
[15] G. Auday, Ph. Guillot, J. Galy, H. Brunet, in Proceedings of the 24th International Conferences on Phenomena in Ionized Gases, Warsaw, Poland, 11–16 July 1999, Vol. IV, pp. 69–70.
[16] R. Veerasingam, R. B. Cambell, and R. T. McGrath, IEEE Trans. Plasma Sci. **23**, 688 (1995).
[17] O. Sahni, C. Lanza, and W. E. Howard, J. Appl. Phys. **49**, 2365 (1978).
[18] Thomson Plasma (private communication).
[19] W. L. Nighan, IEEE Trans. Electron Devices **ED-28**, 625 (1981).